Journal of Materials Chemistry C

Accepted Manuscript

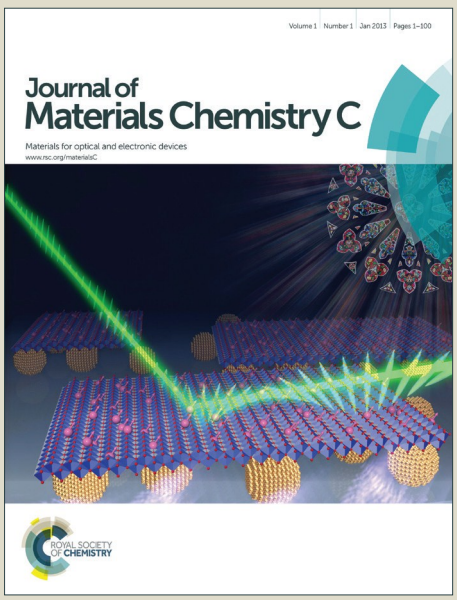

ROYAL SOCIETY OF CHEMISTRY

www.rsc.org/materialsC

Novel Aspects in the Chemistry of the non-Aqueous Fluorolytic Sol-Gel Synthesis of Nanoscaled Homodisperse MgF_2 Sols for Antireflective Coatings

Thoralf Krahl[1,2], Dirk Broßke[1], Kerstin Scheurell[1], Birgit Lintner[3], Erhard Kemnitz[1,2]*

[1] Humboldt-Universität zu Berlin, Brook-Taylor-Str. 2, D-12489 Berlin, GERMANY
[2] Nanofluor GmbH, Rudower Chaussee 29, D-12489 Berlin, GERMANY
[3] Prinz Optics GmbH, Simmernerstr. 7, D-55442 Stromberg, GERMANY
* tel: +49 30 2093 7555, fax: +49 30 2093 7277, mail: erhard.kemnitz@chemie.hu-berlin.de

Abstract
Water-clear transparent sols of *nano*-MgF_2 and *nano*-MgF_2-CaF_2 composites in ethanol were synthesized through the fluorolytic sol-gel synthesis by the reaction of the insoluble precursor magnesium ethoxide with anhydrous hydrogen fluoride. CO_2, $MgCl_2$ or $CaCl_2$ are used as auxiliary reagents. The sols contain monodisperse nanoparticles with a size between 5 and 10 nm, depending on the particular synthesis method used. In contrast to all previous synthesis methods, the sols possess a low viscosity and offer a remarkably high long-time stability for more than one year. It has been demonstrated that they are very suitable for manufacturing antireflective porous coatings on glass substrates with remaining reflectivity below 1%, and high mechanical stability.

1 Introduction

Metal fluorides play an important role for many potential applications. The alkaline earth fluorides, and especially magnesium fluoride, have gained interest due to their superior optical properties. MgF_2 provides a wide optical transmission ranging from short UV (~100 nm) to MIR (~8 µm) and possesses a low refractive index of 1.38.[1] The availability of alkaline earth fluorides as homodispersed nanoparticles opens a wide range of possible materials, e.g. coatings, composites, ceramics and others. So far, most sol–gel systems aim at oxide compositions, the related hydrolysis and condensation reactions have been extensively studied.[2-4] Thin layers of around 100 nm thickness possessing antireflective properties can be synthesized easily from such nanoparticles. The standard procedure for the production of MgF_2 coatings before fluorolytic sol-gel synthesis has been sputtering or evaporation technique.[5, 6] This results in a dense coating layer, and substrates are limited to small size. However, to provide good antireflective properties on glass substrates by a single coating, even the low refractive values of metal fluorides are not low enough to approach 100% transmittance. For this purpose, porosity within the films is required in order to establish a sufficiently low refractive index.[7, 8]

The synthesis of such metal fluoride nanoparticles as transparent sols was developed in our groups during the last years using non-aqueous fluorolytic sol-gel chemistry.[9, 10] The main step is the reaction of a metal precursor with anhydrous hydrogen fluoride (dissolved in alcohol or ether) in non-aqueous solvents, which are alcohols in most cases (Eq. 1).

$$MgX_2 + 2\ HF_{solv} \xrightarrow{(ROH)} \textit{nano}\text{-}MgF_2 + 2\ HX \qquad (1)$$

Several methods for the non-aqueous fluorolytic sols gel synthesis of water-clear sols of *nano*-MgF_2 have been published already.[11-16] These sols contain homodispersed

nanoparticles of a diameter below 20 nm. The usability of these sols, as well as sols synthesized from aqueous routes, has been thoroughly investigated for the production of antireflective λ/4 layers on glass.[13, 16-19] Although a lot of work has been done in this field, there still are several obstacles and drawbacks.

One of the most suitable precursors for this synthesis is magnesium methoxide $Mg(OCH_3)_2$. In methanol, transparent sols of MgF_2 can be obtained. The only byproduct during the sol-gel synthesis is methanol itself. However, the commercially available $Mg(OCH_3)_2$ does not react properly, and therefore, it has to be prepared freshly by the reaction of Mg metal with water-free methanol. Large amounts of hydrogen gas are evolved during this reaction.[11, 12, 14] Furthermore, the reaction can only be carried out in methanol. Attempts to transfer this synthesis to ethanol failed so far due to the insolubility of the magnesium methoxide in ethanol.

Another suitable precursor is magnesium acetate, which is usually traded as tetrahydrate $Mg(CH_3COO)_2{\cdot}4H_2O$. This compound cannot be used directly for the sol-gel synthesis of MgF_2. The acetate has to be dried in vacuum in advance. Drying at ambient pressure is not possible. The so obtained water-free $Mg(CH_3COO)_2$ is suitable for sol-gel synthesis of transparent MgF_2 sols in ethanol, which have been thoroughly investigated for manufacturing antireflective coating on glass.[15, 16] But there is still one disadvantage of this method. Large amounts of acetic acid are formed. The sols have a tang smell, and additionally, acetic acid can react with the solvent ethanol to form acetic ester and water. The water makes the sols unstable on a long-time scale, resulting in increasing viscosity, and finally, gelation after some weeks or months. This is a general problem when using carboxylates as precursors and alcohols as solvent.

Another precursor which has been used is water-free magnesium chloride $MgCl_2$.[13] The sols produced from this precursor are water-clear and stable. Unfortunately, they contain large amounts of water-free hydrogen chloride, which causes corrosion issues.

In the present work, the synthesis of nanoscale magnesium fluoride using an alkoxide as precursor was successfully developed for the solvent ethanol. A suitable precursor for that goal is commercially available magnesium ethoxide $Mg(OEt)_2$ (Et = C_2H_5). Unfortunately, this compound is insoluble in alcohols, and hence all attempts to obtain clear MgF_2 sols from this system failed so far. However, it has been shown that stable solutions of $Mg(OEt)_2$ in ethanol can be obtained when CO_2 is passed though the suspension.[20] The nature of these solutions was not investigated until now. In the present work, such precursor solutions were synthesized, analyzed by NMR and FTIR spectroscopy, and were applied to the synthesis of MgF_2 nanoparticles.

Based on these positive results, a new second approach for the synthesis of transparent *nano*-MgF_2 sols was developed. Instead of using the weak Lewis acid CO_2 as an auxiliary agent, the presence of small *catalytic* amounts of the strong acid HCl during the synthesis, which is formed *in situ* by the reaction of small amounts of $MgCl_2$ and HF, is sufficient. Besides $MgCl_2$, also $CaCl_2$ was used, resulting in the formation of *nano*-MgF_2-CaF_2 composite sols. These sols were characterized by DLS, TEM and NMR spectroscopy.

The suitability of these *nano*-MgF_2-CaF_2 composite sols for manufacturing antireflective coatings on glass is also demonstrated. The stability of the sols and the quality of the coatings were tested over a period of 12 months.

2 Experimental

2.1 Reactants

Reactants used. Pre-dried methanol was obtained from Sigma Aldrich Co. (99.6%). Pre-dried ethanol was obtained from Carl Roth GmbH (K928, 99.8%, denatured with 1% of MEK). This denatured ethanol was used as long as not stated otherwise. Magnesium ethoxide $Mg(OEt)_2$ was obtained from ABCR (95+%). $MgCl_2$ and $MgCl_2 \cdot 6H_2O$ were obtained from Sigma Aldrich. $CaCl_2$ (96%) was obtained from ABCR. The Mg content of $Mg(OEt)_2$ was determined by titration: About 100 – 200 mg (exact weight up to 0.1 mg) of the sample was dissolved in a few milliliters of hydrochloric acid, and then filled up to 100 ml with distilled water. 10 ml of this solution were titrated using 0.01 N ETDA (disodium salt) in NH_3/NH_4Cl buffer using Erio T as indicator.

Production of alcoholic HF. Alcoholic HF was stored in a 1 liter FEP plastic bottle furnished with a Teflon screw cap with three openings for handling under argon. Around 500 – 700 ml of industrially pre-dried alcohol (methanol 99.6% or undenatured ethanol 99.5%) was submitted in the bottle. Gaseous HF mixed with argon was bubbled slowly through the alcohol. Tubes were made of stainless steel and PTFE. The HF bomb was heated up to 60°C to ensure a steady flow of HF. The bottle containing the alcohol was cooled with ice. After 2 – 4 hours around 1 liter of alcoholic HF was obtained. This solution was stored under argon. HF content was determined by titration NaOH using phenolphthalein as indicator. Typical concentrations range from 15 – 30 mol per liter. *Caution: HF is a hazardous agent and has to be used under restricted conditions only.*

2.2 Production of MgF_2 sols and manufacturing of antireflective coatings

Solution of $Mg(OEt)_2$ in alcohol containing CO_2. $Mg(OEt)_2$ in the desired concentration (usually 0.4 M) was dispersed in alcohol (methanol or ethanol). The reaction vessel was closed and equipped with a bubbler. A slow stream of CO_2 was bubbled through the reaction mixture under vigorous stirring. The $Mg(OEt)_2$ usually dissolves within 1 to 2 hours, and hence, a clear solution is obtained. When kept under inert gas (argon), the solution is stable for at least several weeks.

MgF_2 sol, CO_2 method. To the solution described in the previous section, alcoholic HF was added carefully (5 min for 1 liter batch) under vigorous stirring. The exact amount of HF (2.0 eq per Mg) is volumetrically adjusted using equipment made of polypropylene. CO_2 is released forming bubbles. The reaction mixture is stirred for at least one day. *Caution: HF is a hazardous agent and has to be used under restricted conditions only.*

MgF_2 or MgF_2-CaF_2 sol, chloride method. $Mg(OEt)_2$ was dispersed in reaction ethanol. MCl_2 (M = Mg, Ca) was added. The overall metal concentration Mg+M was 0.4 M. This dispersion was stirred for 10 min, in which the MCl_2 usually is dissolved. To this solution, alcoholic HF is added slowly under vigorous stirring. The exact amount of HF (2.0 eq per [Mg+M]) is volumetrically adjusted using equipment made of polypropylene. The reaction mixture is stirred for at least one day.

Antireflective coatings. Float glass (Pilkington Optifloat™, η_{589} = 1.52) and borosilicate glass (Schott Borofloat®, η_{589} = 1.47) of the size 100×200×3 mm were used as substrates. Antireflective coatings were obtained by dip coating of the glass plates

(withdrawal rate 6 mm/s), followed by curing for 15 min at 480°C. *Caution: HF is a hazardous agent and has to be used under restricted conditions only.*

2.3 Analysis

NMR. NMR spectra were recorded on a Bruker Avance 400. ^{1}H and ^{13}C spectra of solutions were recorded using an internal lock tube of C_6D_6 at resonance frequencies of 400 MHz for ^{1}H and 100 MHz for ^{13}C. Chemical shifts were referenced to the signal of the residual proton or the carbon of C_6D_6, respectively ($\delta(^{1}H)$ = 7.16 ppm, $\delta(^{13}C)$ = 128.1 ppm). ^{19}F and ^{27}Al spectra of sols were recorded in a solid state NMR device in 4 mm rotors under static conditions at resonance frequencies of 376 MHz for ^{19}F and 104 MHz for ^{27}Al. The chemical shifts of ^{19}F and ^{27}Al are referenced to external standards of CCl_3F or 1 M aqueous $AlCl_3$ solution, respectively.

DLS. Dynamic light scattering was measured on a Zetasizer Nano using a 630 nm light source. Samples were filtered through a 0.45 µm filter before measurement. The viscosity of each sol was determined for evaluation.

FTIR. FTIR spectra were recorded using a Perking Elmer FTIR 2000 (KBr beam splitter, DTGS detector) in transmission mode. The sample was placed between two slabs of KRS-5 of 3 mm thickness. The background was measured in the same way using the pure solvent (methanol or ethanol).

TEM. TEM images and EDX analysis were recorded using a Philips CM200. For the sample preparation, sols were diluted to 0.1 mM. Droplets of these diluted sols were placed on a carbon coated copper grid (300 mesh, thickness 5-6 nm) and allowed to evaporate.

Reflectance data. Reflectance of coated glass samples was measured on a Zeiss diode array spectrometer. The residual reflectance was determined according to DIN5033 using light D65. Thickness and refractive index of coatings was determined by fitting the reflectance data using the program TFCalc.

Mechanical stability test. Mechanical stability of glass coatings was measured in dependence on DIN 1096-2: In the original norm, a felt piece is cycled 25 times to and fro over the glass with a contact force of 4 N. Instead, for our characterization, coarse steel wool 00 was used. The quality of the coating after the test was determined by comparison with standard samples (see Table 1).

Table 1. Criteria for the judging of the mechanical stability test.

Grade	**Appearance of the coating after mechanical stability test** *coarse steel wool 00, 25 passes, contact pressure 4 N*
1	No scratches
2	Few scratches in the coating, which do not reach the glass.
3	Scratches in the coating, some of them reach the glass.
4	Many scratches in the coating, most of them reach the glass.
5	Coating completely removed.

3 Synthesis – the CO_2 approach

3.1 Preliminary results

Magnesium ethoxide is a moisture sensitive product; however, it is usually distributed in normal glass or plastic bottles. Traces of moisture will cause hydrolysis, and finally, a product of the approximate formula $Mg(OC_2H_5)_{2-x}(OH)_x$ or $Mg(OC_2H_5)_{2-x-y}(OH)_xO_{y/2}$ might be obtained. The theoretical Mg content of $Mg(OEt)_2$ is 21.24%, the Mg content of technical $Mg(OEt)_2$ experimentally determined is 19.78%. It has turned out during the experiments (see next sections) that reactants in different states of partial hydrolysis can be reacted with HF forming a transparent MgF_2 sol, as long as the exact Mg content is known. This is necessary to set up the desired molar ratio of Mg:F.

Upon the reaction of $Mg(OEt)_2$ with 2.0 eq of aqueous or alcoholic HF in methanol or ethanol, an off-white fine precipitate is formed. X-ray diffraction of this powder shows broad reflections of MgF_2 (Figure S1). According to Scherrer's equation, the crystallite size is below 10 nm.

Thus, nanocrystalline MgF_2 is formed, but transparent sols cannot be obtained this way. The particles are strongly linked to each other thus forming agglomerates and aggregates. Chemically, these linkers are strong oxo-bridges, Mg-O-Mg, which are already present in the partially hydrolyzed precursor $Mg(OEt)_2$. The acidity of HF in ethanol is low, thus breaking off these bridges is impossible.

For the formation of free nanoparticles, and hence, the formation of a clear sol, auxiliary reagents are necessary.

3.2 Characterization of precursor solutions

It is known for some time, that either metallic magnesium or magnesium ethoxide can be dissolved in alcohols upon treatment with gaseous CO_2.[20] To understand this process, two test solutions were synthesized for characterization by FTIR and NMR spectroscopy:

- **Prec-01**: 0.4 M solution of $Mg(OEt)_2$ in ethanol by introduction of CO_2
- **Prec-02**: 0.4 M solution of $Mg(OEt)_2$ in methanol by introduction of CO_2

Undenatured ethanol was used for the preparation of Prec-01 to facilitate analysis. The uptake of CO_2 was determined by weight. It is around 1.8 eq related to Mg for both solutions. A picture of the typical appearance of these solutions is shown in Figure 1. The concentration of these solutions can be increased to around 2 mol Mg per liter. Attempts to crystallize the soluble precursor from this solution failed. Only amorphous products containing ~15% carbon were obtained.

Figure 1. Typical precursor solution in the CO_2 method. The cannula in the upper right corner was used for introducing CO_2.

FTIR spectra of the solutions are shown in Figure 2. An intensive band at around 1640 cm^{-1} is observed for both spectra. This band is in the typical range of carbonyl vibrations. It is caused by monosubstituted carbonates $ROCO_2^-$. Only small bands of free CO_2 at 2330 cm^{-1} are observed, and they are derived most probably from the surrounding air. [21]

The signal positions in ^1H and ^{13}C NMR data of these solutions are given in Table 2. In the case of Prec-01 (solution in ethanol), two different ethyl groups can be identified. Two large signals of the solvent ethanol are observed, and additionally, two small signals, which are interpreted as signals of monoethylcarbonate $C_2H_5OCO_2^-$. The ^{13}C NMR shift of the carbonyl group at 160.5 ppm is in the typical range of carbonates, e.g. dialkyl carbonates $(RO)_2CO$ ~156 ppm.[22] No signal of free CO_2 at 125 ppm is observed.[23] For Prec-02 (solution in methanol) the NMR spectra are appropriate. Beside the intensive signal of the solvent methanol, no monoethylcarbonate $C_2H_5OCO_2^-$ is observed, but only monomethylcarbonate $CH_3OCO_2^-$. Consequently, small amounts of free ethanol are found.

Thus, it is evident the CO_2 has reacted with the magnesium ethoxide, and furthermore, has formed a soluble species of magnesium alkylcarbonate $Mg(ROCO_2)_2$ (R = CH_3, C_2H_5).

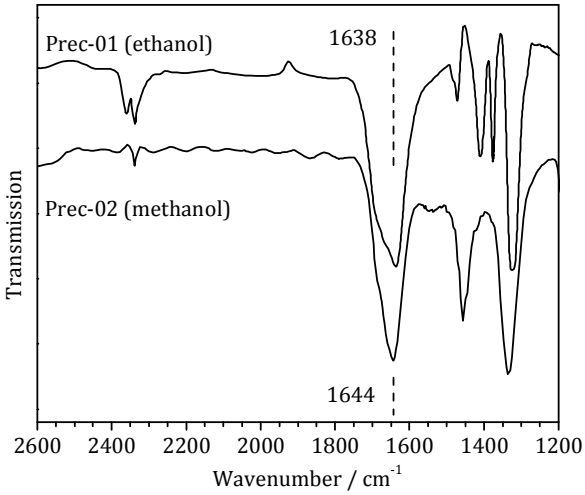

Figure 2. FTIR spectra of precursor solutions ($Mg(OEt)_2$ in alcohol with CO_2).

Table 2. NMR spectra of solutions of $Mg(OEt)_2$ in CO_2-containing alcohols. (*) undenatured

Reaction	^{13}C NMR / ppm	Species	^{1}H NMR / ppm	Species
Prec-01 $Mg(OEt)_2 + CO_2$ in ethanol(*)	15.1	$\boldsymbol{C}H_3CH_2OCO_2^-$	1.73 (*t*)	$\boldsymbol{C}H_3CH_2OCO_2^-$
	62.3	$CH_3\boldsymbol{C}H_2OCO_2^-$	4.52 (*q*)	$CH_3C\boldsymbol{H}_2OCO_2^-$
	160.2	$CH_3CH_2O\boldsymbol{C}O_2^-$		
solvent	18.3	$\boldsymbol{C}H_3CH_2OH$	1.70 (*t*)	$C\boldsymbol{H}_3CH_2OH$
	57.8	$CH_3\boldsymbol{C}H_2OH$	4.14 (*q*)	$CH_3C\boldsymbol{H}_2OH$
			5.98 (*s*, br)	RO***H***
Prec-02 $Mg(OEt)_2 + CO_2$ in methanol	18.1	$\boldsymbol{C}H_3CH_2OH$	1.87 (*t*)	$C\boldsymbol{H}_3CH_2OH$
	53.6	$\boldsymbol{C}H_3OCO_2^-$	4.27 (*s*)	$C\boldsymbol{H}_3OCO_2^-$
	58.2	$CH_3\boldsymbol{C}H_2OH$	4.30 (*q*)	$CH_3C\boldsymbol{H}_2OH$
	161.1	$CH_3O\boldsymbol{C}O_2^-$		
solvent	47.7	$\boldsymbol{C}H_3OH$	4.05 (*s*)	$C\boldsymbol{H}_3OH$
			5.79 (*s*, br)	RO***H***

3.3 Synthesis and characterization of MgF_2 Sols

Such precursor solutions were reacted with alcoholic HF solutions. In general, water-clear solutions can only be obtained, when the concentration of Mg does not exceed 0.2 M. Higher concentration of Mg leads to the formation of turbid sols. An overview over the synthesized sols is given in Table 3.

Table 3. Overview over MgF_2 sols synthesized according to the CO_2 method. (MeOH = methanol; EtOH = ethanol; TFA = CF_3COOH; % is mol-% relative to Mg)

Nr.	Conc. & solvent	HF	Additive	Sol after synthesis	DLS diameter
Sol-C01	0.2 M in methanol	2.0 eq HF/MeOH		0 d: turbid 3 d: clear	$d_{max} \approx 4$ nm
Sol-C02	0.2 M in ethanol	2.0 eq HF/MeOH		0 d: turbid 3 d: turbid	
Sol-C03	0.2 M in ethanol	2.0 eq HF/MeOH	20% TFA	0 d: turbid 3 d: clear	$d_{max} \approx 9$ nm
Sol-C04	0.2 M in 98% ethanol + 2% methanol	2.0 eq HF/EtOH	20% TFA	0 d: turbid 3 d: turbid	
Sol-C05	0.2 M in ethanol	2.0 eq HF/EtOH	20% TFA	0 d: turbid 3 d: turbid	

Upon fluorination, all sols release CO_2. Therefore, the fluorination should be carried out carefully to avoid overboiling. In all cases, turbid sols are formed immediately after fluorination.

Fluorination of a precursor solution in methanol with methanolic HF leads to the formation of clear sols within 3 days (Sol-C01). This synthesis is straightforward and reproducible.

Initial trials to reproduce the synthesis in ethanol failed. Only turbid sols were obtained. It is well known from previous results that the addition of trifluoroacetic acid (TFA) leads to deagglomeration and stabilization of the nanoparticles.[12] This stabilizer was also tested here in different combinations. Fluorination of a precursor solution in *ethanol* with *methanolic* HF lead to the formation of a turbid sol (Sol-C02), which cleared off 3 days after addition of TFA (Sol-C03). Sol-C03 then contains ~2% methanol. Attempts to add the methanol to the precursor solution and using *ethanolic* HF lead only to the formation of turbid sol, even when adding TFA (Sol-C04), although the overall composition of Sol-C03 and Sol-C04 is the same. Furthermore, the fluorination of the precursor solution in *ethanol* with *ethanolic* HF also leads to the formation of turbid sols only, even when large amounts (>20 mol-%) of TFA were added.

The DLS data of both clear sols (Sol-C01 and Sol-C03) are given in Figure 3. The MgF_2 particles in the methanolic Sol-C01 have a hydrodynamic diameter of 4 nm. The size distribution is slightly asymmetric. In contrast to that, the particles in the ethanolic Sol-C03 are larger, having a hydrodynamic diameter of 9 nm.

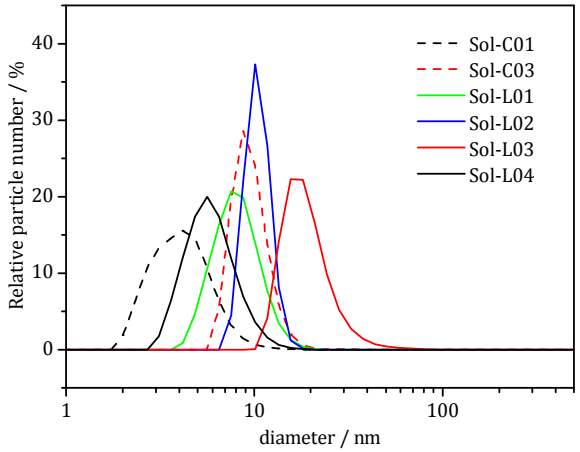

Figure 3. DLS data (number of particles) of different sols.

4 Synthesis – the chloride approach

4.1 Motivation

As seen in the previous section, CO_2 can be used successfully to enhance the reactivity of insoluble $Mg(EtO)_2$. It was shown that this effect is caused by the formation of monoesters of carbonic acid, and hence, CO_2 is able to dissolve $Mg(EtO)_2$. Soluble magnesium monoethylcarbonate $Mg(EtOCO_2)_2$ is formed, which can properly react with HF, thus resulting in the formation of clear monodispersed MgF_2 sols. Consequently, other acids, either Lewis or Brønsted, could have a similar effect. Moreover, a strong acid should be sufficient in catalytic amounts instead of the stoichiometric amounts of CO_2.

Hydrogen chloride HCl is a much stronger acid than HF and monoethylcarbonic acid, and therefore it is a potential auxiliary reagent. A first attempt of the fluorination of $Mg(OEt)_2$ with methanolic HF in methanol in the presence of ≈10 mol-% (related to Mg) concentrated hydrochloric acid was promising. Sols were obtained instead of precipitates. However, the sols were not water-clear but turbid, and underwent gelation after one week. The reason for that behavior is obvious. Concentrated hydrochloric acid contains a certain amount of water (molar ratio H_2O:HCl ≈3.5). It is known from many previous experiments that water will cause the primary particles to agglomerate, and prevent them from the formation of clear sols.

4.2 Synthesis of MgF_2 sols

The use of water free hydrogen chloride would overcome the problem with the gelatinization of the sol due to the presence of water. Since water-free hydrogen chloride is difficult to handle, we worked out a way to produce HCl *in situ* during the reaction by adding water-free metal chlorides.

Adding 10 mol-% of water-free $MgCl_2$ to a suspension of $Mg(OEt)_2$ in ethanol, followed by the reaction with small amounts of anhydrous HF, forms MgF_2 and water-free HCl in a first step.

The fluorination of such a mixture of $Mg(OEt)_2$ and $MgCl_2$ in ethanol with not only a small amount of HF, but the necessary 2 equivalents of alcoholic HF solution in one batch, leads directly to the formation of clear sols of MgF_2 (see Table 4 Sol-L01 and Sol-L02). Interestingly, when *methanolic* HF (Sol-L01) is used, clear sols can be obtained within 1 hour. In the case of *ethanolic* HF (Sol-L02), the sols need some hours to clear off. This behavior is similar to that observed in the CO_2 method.

In order to probe the effect of water, one test was carried out using $MgCl_2 \cdot 6H_2O$ instead of water free $MgCl_2$. This sol (Sol-L03) clears off very fast. The small amount of crystal water seems to increase the reactivity of the whole system. However, expectedly these sols are not long-time stable. The viscosity rapidly increases within 2 weeks.

Furthermore, $CaCl_2$ was used as chloride source (Sol-L04) instead of $MgCl_2$. Calcium fluoride CaF_2 should be formed besides MgF_2. Also with $CaCl_2$, water-clear sols are formed, but the sols clear off slower than in the case of $MgCl_2$.

The amount of chloride used for the synthesis was varied from 5 to 30 mol-% of the total Mg content (Sol-L05 and Sol-L06). When only 5 mol-% of the chloride source is used, the sols clear off only within a few days. Vigorous stirring decreases the clearing time. When 15% are used, the time for clearing-off is already greatly decreased (Sol-L05). Finally, when using 30 mol-% of the chloride source, the sols are clear nearly instantly after the addition of HF to the precursors (Sol-L06).

The particle diameters of the water-free sols are all below 10 nm (see Figure 3 and Table 4). The smaller particle size of Sol-L04 (containing calcium) compared to Sol-L02 (the same sol without calcium) is noteworthy. In the case of the water-containing Sol-L03, the particle size has nearly doubled to an amount of 17 nm.

Table 4. Overview over MgF_2 sols synthesized according to the chloride method (conc relates to the total amount Mg+Ca, % is mol-% of total amount Mg+Ca, d_{max} ~ particle diameter from DLS maximum, η ~ viscosity).

Nr.	Conc. & solvent	Reactants	HF	Sol after synthesis	DLS data (relative number)
Sol-L01	0.4 M in ethanol	90% $Mg(OEt)_2$ 10% $MgCl_2$	2.0 eq HF/MeOH	clear after 1 h	d_{max} ≈ 8 nm η = 1.187 mPa·s
Sol-L02	0.4 M in ethanol	90% $Mg(OEt)_2$ 10% $MgCl_2$	2.0 eq HF/EtOH	clear after 6 h	d_{max} ≈ 9 nm η = 1.200 mPa·s
Sol-L03(*)	0.4 M in ethanol	90% $Mg(OEt)_2$ 10% $MgCl_2{\cdot}6H_2O$	2.0 eq HF/EtOH	clear after 6 h	d_{max} ≈ 17 nm η = 1.483 mPa·s
Sol-L04	0.4 M in ethanol	90% $Mg(OEt)_2$ 10% $CaCl_2$	2.0 eq HF/EtOH	clear after 15 h	d_{max} ≈ 6 nm η = 1.190 mPa·s
Sol-L05(#)	0.4 M in ethanol	85% $Mg(OEt)_2$ 15% $CaCl_2$	2.0 eq HF/EtOH	clear after 2 h	d_{max} ≈ 5 nm η = 1.118 mPa·s
Sol-L06	0.4 M in ethanol	70% $Mg(OEt)_2$ 30% $CaCl_2$	2.0 eq HF/EtOH	clear after 10 min	

(*) This sol is not stable for more than 2 weeks. The viscosity increases rapidly.

(#) Sol-L05A: 3 mol-% $Al(O^iPr)_3$ added after synthesis (^iPr = *iso*-C_3H_7)

TEM images are presented in Figure 4. In general, the contrast of such small MgF_2 particles or MgF_2-CaF_2 composites is low due to the low scattering intensity of the light Mg and F atoms (A and B). Further, the particles show a beam sensitive behavior and change during exposure to the electron beam. In high resolution mode, MgF_2 particles can be identified by their lattice spacing of 2.23 Å (C). EDX analysis of the measured particles is given in the supporting information (Figure S2).

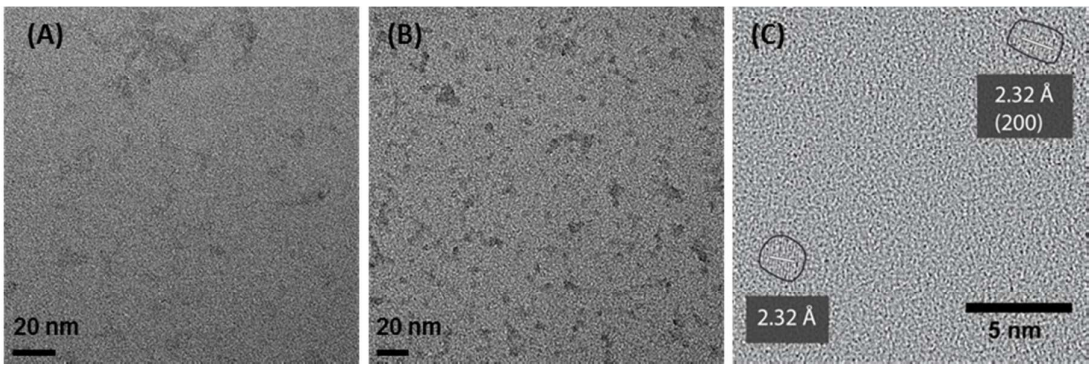

Figure 4. TEM images of particles from evaporated sols (A) Sol-L02, (B) Sol-L04, (C) high resolution of Sol-L01.

4.3 NMR spectroscopy of sols containing calcium

Further evidence of the occurrence of nanoparticles is given by ^{19}F NMR spectroscopy. Dispersed nanoparticles show liquid-like spectra with broad *isotropic* lines (fwhm ~1…2 kHz) due to the motion of the particles in the solution.[14] This is in contrast to solids, where *anisotropic* lines are observed, and also in contrast to real solutions, where very narrow isotropic signals are observed. The chemical nature of the particles of the pure MgF_2 sols (Sol-L01…L04) can be clarified by the chemical shift of -198 ppm, which corresponds to MgF_2. An example for Sol-L02 is given in the supporting information (Figure S3), showing a broad isotropic signal at -198 ppm in ^{19}F NMR with a line width of 1.6 kHz.

The chemical nature of the MgF_2-CaF_2 composites was studied in more detail. The crystal structures of MgF_2 (rutile) and CaF_2 (fluorite) are different from each other. The formation of solid solutions between both of the compounds was never observed.[24] The ^{19}F NMR spectra of Sol-05 and Sol-06 containing 15 and 30 mol-% calcium, respectively, are presented in Figure 5. Both spectra show the typical broad isotropic signals of nanoparticles. CaF_2 (-108 ppm) and MgF_2 (-198 ppm) can be clearly identified. The signal of MgF_2 at -198 ppm is asymmetric with more intensity on the high field side. This signal shape is typical for magnesium fluoride, which is not fully fluorinated, but contains oxo-species.[14, 25] Additionally, some broad signals occur between these both lines, and a narrow signal at -178 ppm. This small signal is due to traces of remaining HF, which is adsorbed at the particles surface.

Interestingly, the intensity of the signal of CaF_2 is much lower than expected. This can be explained by the formation of the metastable phase $CaMgF_4$. The formation of this phase was already observed during mechanosynthesis of mixed fluorides using Mg and Ca precursors simultaneously and ammonium fluoride as fluorinating agent.[24] Theoretically, the spectrum consists of 24 independent lines. Amorphous and nanoscale samples show only two broad signals with maxima at around -140 and -170 ppm. A schematic deconvolution of the spectra is also given in Figure 5.

In fact, the MgF_2-CaF_2 nanocomposites consist of three different phases, namely MgF_2, CaF_2 and $CaMgF_4$. Thus, the low intensity of the CaF_2 NMR signal can be fully explained by the formation of $CaMgF_4$. It is known from previous experiments that this phase is metastable, and it will decompose into MgF_2 and CaF_2 upon thermal treatment. This behavior has to be kept in mind for further applications.

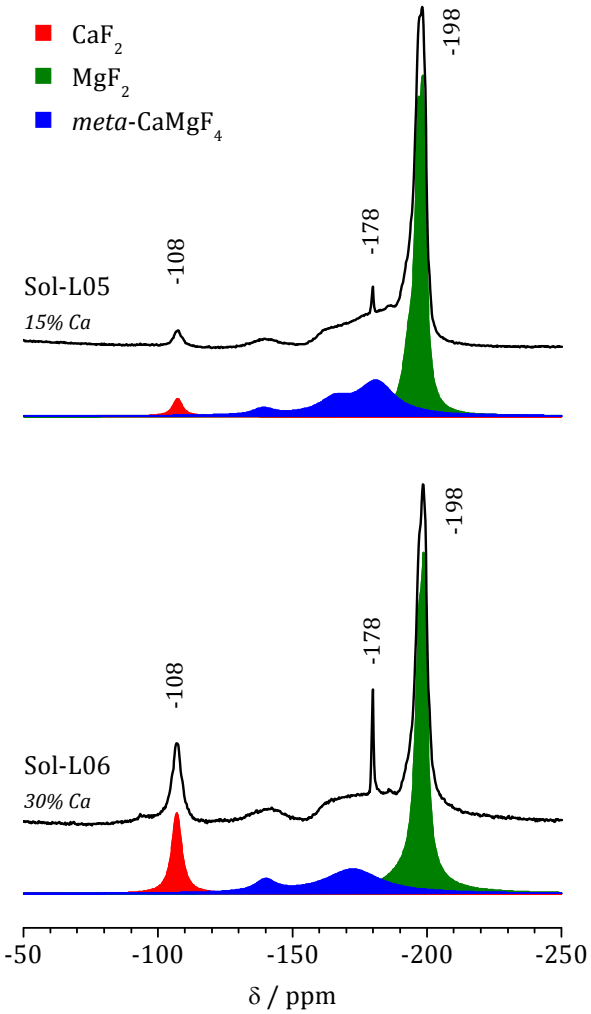

Figure 5. ^{19}F NMR spectra of Sol-L05 and Sol-L06.The schematic deconvolution is shown colored. The signal at -178 ppm is due to traces of adsorbed HF.

5 Discussion

5.1 Precursor activation

The direct fluorination of $Mg(OEt)_2$ with anhydrous HF in an alcoholic reaction medium does not deliver a sol of nanoscale MgF_2 particles, but will always lead to the formation of precipitates (see e.g. Figure S1). There are two reasons for that. On the one hand, magnesium ethoxide $Mg(OEt)_2$ is insoluble in alcohols, and hence, instead of a homogenous reaction a heterogeneous reaction takes place forming a protecting MgF_2 layer on the outer sphere of the Mg-precursor. On the other hand, products not handled completely under exclusion of moisture are partially hydrolyzed, and therefore, contain hydroxide groups and also strong Mg-O-Mg bridges. The acidity of HF in organic solvents is not high enough to destroy these bridges. Auxiliary agents are needed to increase the reactivity.

One possible reagent is CO_2. It is able to form monoethylcarbonic acid and thus can finally form soluble alkylcarbonates. This behavior is well-known for the alkoxides of the alkali metals and thallium.[21] The crystal structures of the sodium and potassium monomethylcarbonate are known.[26, 27] The same reaction takes place, when CO_2 is passed through a suspension of $Mg(OEt)_2$ in ethanol. For the ideal case, this reaction is:

$$Mg(C_2H_5O)_2 + 2\ CO_2 \xrightarrow{EtOH} Mg(C_2H_5OCO_2)_2 \qquad (2)$$

Formally, the key step is the nucleophilic attack of an alkoxide ($RO^- = CH_3O^-, C_2H_5O^-$) at the weak electrophile (or weak Lewis acid) CO_2:

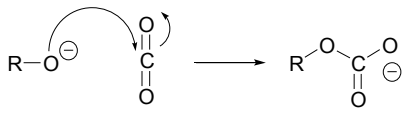

The important fact is that this reaction takes place also with the insoluble $Mg(OEt)_2$ or a partially hydrolyzed $Mg(OEt)_{2-x}(OH)_x$, thus forming a *soluble* intermediate, resulting in clear precursor solutions. Nearly 2 equivalents of CO_2 are taken up by $Mg(OEt)_2$. The solubility of the precursors is an important first step in the formation of clear sols of nanoparticles. The formation of ethylcarbonate has been proven by NMR and IR spectroscopy. In the case of methanol as solvent, methylcarbonate is formed instead of ethylcarbonate, but the discussion of the phenomena can be adopted analogously. In contrast to the alkylcarbonates of Na and K, the stability of the non-solvated Mg compound is low. All attempts to crystallize $Mg(C_2H_5OCO_2)_2$ failed, and resulted in a decomposition of the product.

The formation of disubstituted carbonates $(RO)_2CO$ can be excluded. The degree of substitution of a carbonate can be differentiated by the asymmetric $\nu_{as}(CO_3)$ valence vibration band in the FTIR spectrum. Disubstituted carbonates $(RO)_2CO$ show this band at ~1750 cm^{-1},[22] monosubstituted carbonates $ROCO_2^-$ at ~1650 cm^{-1},[21] while the free carbonate ion CO_3^{2-} has this band at ~1450 cm^{-1}.[28] The strong IR band of the precursor solutions is found at ~1640 cm^{-1}, and hence, both the FTIR spectra (Figure 2) and the NMR spectra (Table 2) proof the formation of monoalkylcarbonates.

Surprisingly, also the partially hydrolyzed product does dissolve completely during the introduction of CO_2. Oxo-bridges and hydroxyl groups can react with the CO_2, more probably with intermediately formed monoethylcarbonic acid, to form carbonate CO_3^{2-} and hydrogen carbonate HCO_3^-. Obviously, partial hydrolysis of the reactant $Mg(OEt)_2$ does not disturb the formation of clear precursor solutions.

During fluorination, the free acid $C_2H_5OCO_2H$ is formed. This acid is unstable and immediately decomposes into ethanol and CO_2. The same accounts for HCO_3^- and CO_3^{2-}. Upon protonation, carbonic acid is formed, which decomposes into H_2O and CO_2. A schematic overview about the reactions in this system is given in Figure 6.

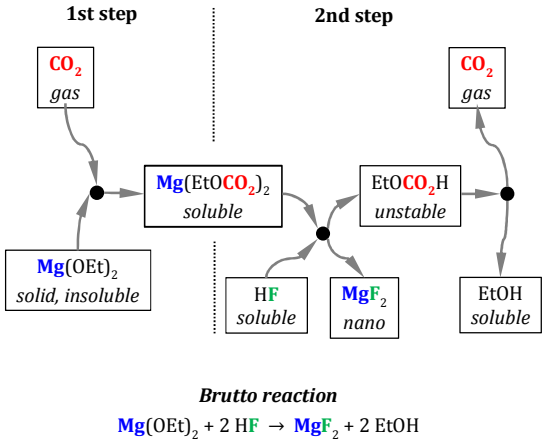

Figure 6. Schematic representation of the reactions occurring during synthesis using the CO_2 method (Et = C_2H_5). Both steps are carried out separately.

Although the synthesis of these clear MgF_2 sols was quite successful, this method still has several disadvantages: (i) Stoichiometric amounts of CO_2 are necessary, (ii) the reaction requires two steps to be carried out separately, and (iii) the maximum concentration of 0.2 M MgF_2 (i.e. 12 g/l) is quite low. To overcome these drawbacks, but taking into account the same chemical principle an easier but more efficient method was developed.

The role of CO_2 is formally that of a Lewis acid, which breaks the strong oxo-bridges in the solid $Mg(OEt)_2$. Other acids, and especially strong acids, should have the same effect. Hydrogen chloride is a very strong acid, and hence, is able to protonate hydroxyl groups, and also to break Mg-O-Mg bonds. Upon reaction of HCl with $Mg(OEt)_2$, soluble $MgCl_2$ is formed. When HF is present in the reaction mixture, $MgCl_2$ will react immediately with it to form nanoscale MgF_2, thus forming HCl again. This HCl can react with still unreacted $Mg(OEt)_2$, and hence, a catalytic cycle is established.

This whole process can be carried out in one step in a one-pot reaction. $MgCl_2$ and $Mg(OEt)_2$ are provided in ethanol. The $MgCl_2$ will quickly dissolve in alcohol, while the $Mg(OEt)_2$ remains as a solid. Upon fluorination, this dissolved $MgCl_2$ will be fluorinated first, HCl is formed beside MgF_2, and the catalytic cycle starts. The same reaction is possible when using $CaCl_2$ as a chloride source, which is also soluble in ethanol. A schematic overview about these reactions is given in Figure 7. The main advantage of the chloride method is the fact that only catalytic amounts of metal chloride or HCl are necessary.

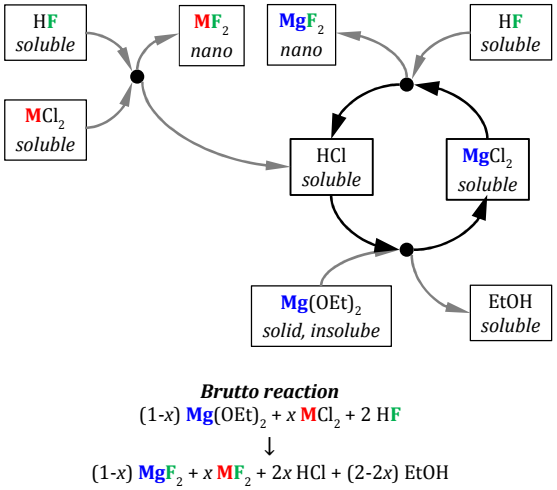

Figure 7. Schematic representation of the reactions occurring during the one-pot synthesis using the chloride method (M = Mg, Ca; x = 0.05...0.30; Et = C_2H_5).

In this way, water-clear MgF_2 sols can be formed in ethanolic solution. No methanol is needed anymore here, and the concentration is higher than in the case of the CO_2 method. Test reactions up to a concentration of 1 M MgF_2 still resulted in transparent sols. Both facts make the sols more suitable for applications. There is one slight disadvantage: These sols are acidic, because they always contain small amounts of HCl. Nevertheless, they are still much less acidic than sols synthesizes from pure $MgCl_2$. It is noteworthy mentioning that state of the oxide sols, e.g. SiO_2 sol, contain similar amounts of acids resulting from the acid catalyzed hydrolysis reaction.

Surprisingly, all sols show a yellow color (Figure 9). It results from impurities of the technical grade reactant $Mg(OEt)_2$. For coating applications, this color does not disturb.

5.2 Reactivity of HF

An interesting fact was observed for both methods. When working in ethanol as a solvent, the fluorination of the precursor with *methanolic* HF will produce clear sols faster and easier than the fluorination with *ethanolic* HF. For that, compare e.g. Sol-C03 and Sol-C05, or Sol-L01 and Sol-L02. A small amount of methanol seems to increase the reactivity. Surprisingly, when a small amount of methanol is added before the fluorination, and then, the fluorination is carried out afterwards with ethanolic HF, no effect of the methanol is observed. Such sols behave in the same way as sols synthesized without methanol. For that, compare Sol-C03 and Sol-C04. Both sols have the same composition and contain the same amounts of methanol. For Sol-C03, the methanol was added together with HF, and this sol became clear. For Sol-C04, the methanol was added to the precursor solution before the fluorination, and this sol remained turbid.

The most plausible explanation of this behavior is the different reaction speed of the initial nucleation in both systems. The reaction between HF and dissolved metal precursor species is fast. It will take place at the interface between the HF droplet and the dissolved precursor. When using methanolic HF, the concentration of methanol at this interface is high (Figure 8). Methanol has a higher polarity than ethanol, and it will

solvate polar species better. Therefore, the initially formed MgF_2 nuclei have fewer tendencies to form agglomerates in methanol, and further, less agglomerated species are formed during the later nucleus growth. This results in a lower degree of agglomeration of the primary particles, and hence, the deagglomeration process is faster.

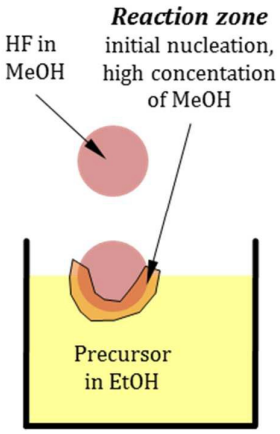

Figure 8. Explanation of the formation of different nuclei when using a solution of HF in methanol.

5.3 Effect of calcium in the chloride approach

As a variation of the chloride approach, $CaCl_2$ can be used instead of $MgCl_2$. These *nano*-MgF_2-CaF_2 composite sols are also monodisperse, although they contain several different compounds (MgF_2, CaF_2 and *meta*-$CaMgF_4$). The clearing of the sols takes more time than in the case of $MgCl_2$. However, there are several advantages using $CaCl_2$: (i) the particle size, i.e. the hydrodynamic diameter, is smaller than in the case of pure MgF_2, and (ii) $CaCl_2$ is less susceptible to hydrolysis at air than MgF_2. These mixed MgF_2-CaF_2 sols offer a broader range of variable parameters.

The reasons for the smaller particle diameter are not fully understood yet. It can be taken for sure that the soluble chloride ($MgCl_2$ or $CaCl_2$) will react first with HF. Both chlorides exhibit a different reactivity towards HF. The initially formed nuclei, namely MgF_2 and CaF_2, have different sizes. This will also cause different particle sizes. This may also be the reason, why the calcium containing sol needs more time to clear off. Due to the smaller diameter, the number of primary particles is higher, and hence, they need more time to deagglomerate.

The use of calcium allows varying the composition of the sols over a certain range. $MgCl_2$, $CaCl_2$ or a mixture of both can be used. Interestingly, the use of $CaCl_2$ instead of $MgCl_2$ greatly improves the mechanical stability of antireflective coatings on glass manufactured from these sols (see next chapter).

5.4 Long-time stability of the sols

All sols, except Sol-L03, synthesized in this work (see and Table 4) are of low viscosity (η < 1.5 mPa·s). When stored closed, they are stable for at least one year without becoming turbid and without increasing their viscosity.

The reason for the high stability of the sols is the absence of large amounts of water, which would cause crosslinking of the particles. Nanoparticles are not thermo-

dynamically stable systems. They need some kind of kinetic stabilization, to prevent them from agglomeration or gelation. In this case, the sols remain with a low viscosity over a certain period of time. Ideally, the solvent itself is the stabilizing agent.

In general, the gelation of sols is caused by adsorption of water on the particles surface, followed by condensation of OH groups. Small amounts of water are already present in the solvent, and some more water may also be formed during the synthesis from partially hydrolyzed $Mg(OEt)_2$. These small amounts of water are not disturbing, and more water is not formed in the sols after the synthesis.

The crucial point here is the absence of carboxylic acids. Note the difference between the synthesis presented here and the known synthesis from magnesium acetate. MgF_2 sols synthesized from magnesium acetate contain acetic acid. Even after the synthesis of the MgF_2 sols is finished, the acetic acid will slowly react with the solvent ethanol to form ethyl acetate and water. Over a certain time of several weeks or months, up to two equivalents of water per Mg can be formed in this way. This gradually increases the sol's viscosity, which finally results in gelation. This fact makes the acetate based sols unstable even when closed from humidity. [15, 16] Sols synthesized from aqueous hydrofluoric acids published by other workgroups will also not be stable over a long-time period.[17-19]

This mechanism of the gradual generation of water in the sols cannot take place in the sols presented in this publication, and hence, the sols are stable on a long-time scale. They will only gelatinize when exposed to (moist) air for longer time, with the exception of Sol-L03. Sol-L03, which already contains water, will gelatinize even when not exposed to air.

5.5 Upscaling of the synthesis

The chloride method as a one-pot reaction is very capable for upscaling. An example of a 5 liter batch is shown in Figure 9. The reaction heat can be handled by slow addition of HF. As a typical example, for a of Sol-L05, HF in ethanol ($c \approx 12$ M) is added to the reaction mixture ($Mg(OEt)_2$+$CaCl_2$) over a time of 15 min. After all HF has been added, the sol is almost clear off (but still not water-clear). After stirring for 1 day water-clear sols are obtained.

The synthesis according to the CO_2 method was also upscaled to a batch of 5 L. Clear sols are obtained within a few days.

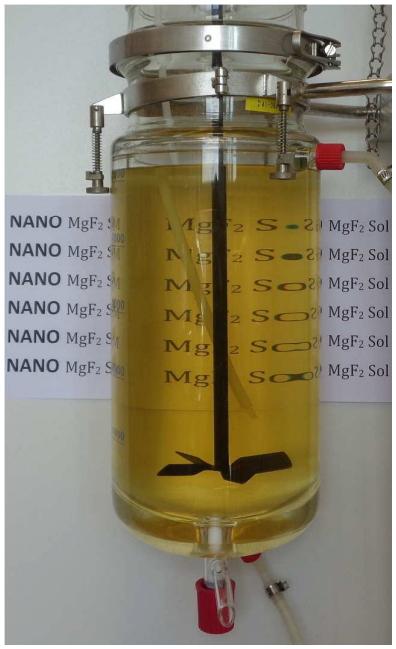

Figure 9. Upscaling – a 5 liter batch of Sol-L05 (0.4 M sol of MgF_2-CaF_2 85:15 in ethanol) 1 day after synthesis. The inner diameter of the reactor is 15 cm.

6 Antireflective coatings on glass substrates

6.1 Preparation of the sol

Based on magnesium fluoride sols thin antireflecting coatings on flat glass substrates can be manufactured by dip coating.[13, 16, 17] Preliminary tests with the sols L01…L06 (Table 4) revealed that antireflective coatings produced using *nano*-MgF_2-CaF_2 composite sols (L04…L06) had a better mechanical stability than those produced from a pure *nano*-MgF_2 sol (L01...02). The optimum CaF_2 content turned out to be around 15 mol-%. Sols with a higher Ca content contain too much HCl, which results in corrosion problems and incomplete wetting of the glass planes. Sols with a lower Ca content resulted in coatings with a poor mechanical stability.

Therefore, a modified sol named Sol-L05A was used for a long time test. This sol contained 85 mol-% MgF_2 and 15 mol-% CaF_2. As difference to Sol-05, 3 mol-% of $Al(O^iPr)_3$ (relative to Mg+Ca, ^{i}Pr = *iso*-C_3H_7) was added immediately after synthesis. It is known from previous work that such additives can greatly increase the stability of these sols and hinder the gelatinization.[15] Compared to Sol-05, the modified Sol-05A showed much less tendency towards gelatinization when handled at open air over a time period of one year..

This surprising stability of the Sol-05A is caused by the additive $Al(O^iPr)_3$, which will first react with the remaining HCl to form $AlCl_3$. At this moment we speculate that hydrated aluminum species like e.g. $[Al(H_2O)_nCl_{6-n}]^{n-3}$ are formed upon exposure to moisture, which can react with traces of HF to form $[Al(H_2O)_nF_{6-n}]^{n-3}$. ^{19}F and ^{27}Al NMR spectra of Sol-05A support this interpretation. In ^{19}F NMR (Figure S4), on top of the broad signal of $CaMgF_4$, another small broad signal occurs at -175 ppm with a half width of ~2 kHz. The chemical shift is typical for octahedrally coordinated AlO_xF_y species. Obviously, some of

the $Al(O^iPr)_3$ forms fluorinated species. These species are adsorbed at the particles surface, which can be concluded from the broadness of the line. In the ^{27}Al NMR spectrum, a faint line occurs at -6 ppm with a width of ~1.9 kHz (Figure S5). The chemical shift of this line is also typical for octahedrally coordinated AlO_xF_y.

HCl is still present in the sol, and hence, the sol is still acidic. In such a solution, the tendency for condensation reactions of the aluminum species, and hence, for the formation of particles like $Al(OH)_3$, AlOOH or Al_2O_3 is low. This will only occur when the amount of water drastically rises up. Therefore, the aluminum compound acts as an "absorber" for moisture, which will otherwise be absorbed at the surface of the nanoparticles to cause gelatinization.

6.2 Optical properties

The sol was tested for coating of flat glass substrates over a period of a whole year. Every month coatings were prepared from the same batch of sol. Transparent coatings on different glass samples were manufactured by dip coating, followed by thermal treatment (see experimental section for details). The reflectance curves are given in Figure 10. The coatings have a thickness of 113 nm and a refractive index of 1.26. The residual reflectance is well below 1% for float glass, and ~1% for borosilicate glass.

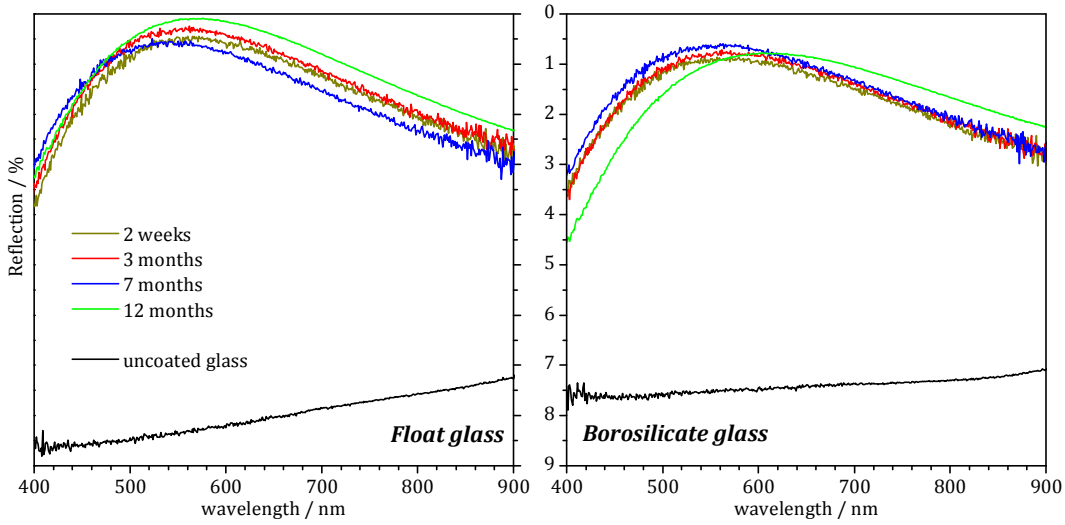

Figure 10. Reflection of coated glass samples using aged Sol-05A.

To demonstrate the effect visually, photographs of coated and uncoated samples are shown in Figure 11. It can be clearly seen that the reflections are greatly reduced for the coated areas, and further, that the transmission of these coated areas is higher.

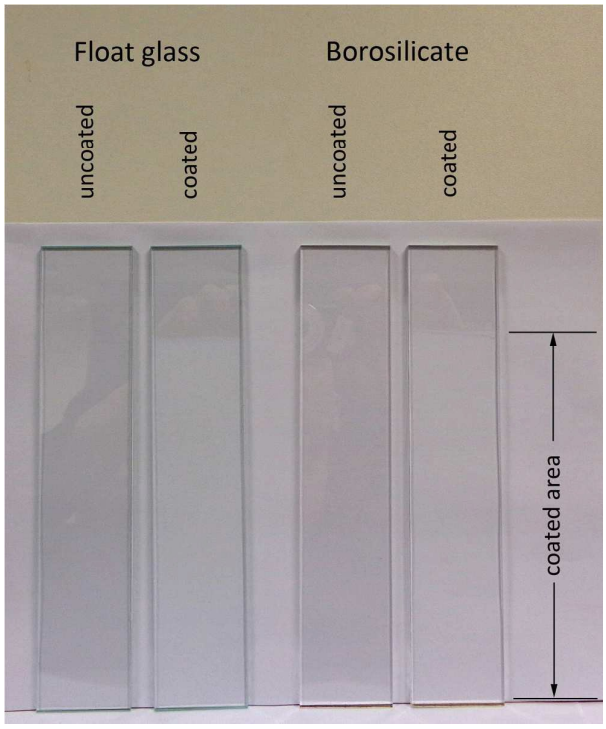

Figure 11. Photographs of coated and uncoated glass substrates.

The excellent antireflective properties of the coatings are caused by their low refractive index. It can be explained by the porosity of the coatings. In theory, the best anti-reflective properties using only one layer are achieved, when the coating layer has at thickness $d_{\text{layer}} = \lambda/4$, i.e. a quarter of the wavelength of the light, and a refractive index of $\eta_{\text{layer}} = \sqrt{\eta}$, i.e. the square-root of the refractive index of the glass.[7] For an effective antireflection, the coating should have a thickness of around 125 nm and a refractive index of ~1.23. The refractive index of pure MgF_2 is η_{500} = 1.38,[1] while that of CaF_2 is η_{500} = 1.44.[29] The refractive index of the coating is usually lower due to the porosity of the coating layer. This porosity is formed during the curing process by evaporation of strongly bound organic molecules. During thermal curing of the coatings, besides the formation of MgF_2 and CaF_2, some Al_2O_3 will be formed due to hydrolysis of the aluminum species. Hence, the final coating layer has a composition of MgF_2:CaF_2:Al_2O_3 in the weight ratio 80.0:17.7:2.3 and the volume ratio 80.3:17.8:1.9. A dense material of this composition has a refractive index of 1.40. Since the coating is porous, the refraction index is much lower, namely 1.26.

Expectedly, the residual reflectance of the coated borosilicate glass is slightly higher than that of coated float glass. The reason for that is the lower refractive index of borosilicate glass. The float glass used here has a refractive index of 1.52. For the ideal λ/4 antireflective layer, the refractive index of the coating should be $\sqrt{1.52} \approx 1.23$. For borosilicate glass the ideal refractive index of the coating layer would be $\sqrt{1.47} \approx 1.21$. Thus, the refractive index of the layers on borosilicate glass is more off the ideal value than for float glass, and therefore, the antireflective properties for borosilicate glass are not as perfect as for float glass, but still exciting.

6.3 Mechanical properties

Usually, the mechanical stability of porous coating is quite poor. Hence, there is no publication about MgF_2 coatings from sols giving any information about the mechanical properties of such AR-layers. However, here we tested the mechanical stability of the MgF_2-coatings by a crockmeter from Erichsen (scratchmarker 249) using felt and steel wool with a fineness of 0000. The stamp with a contact area of 4.5 cm^2 was pressed on the sample with a force of 4 N. "State of the art" MgF_2-layers obtained from magnesium acetate as precursor (as recently described by us [15,16]) show even with felt wool rubber evident scratches but using steel wool rubber the layers were completely removed (cf. Fig. S6a and B) In contrast, MgF_2-layers obtained from Mg-ethoxide sols, as described here, are even resistant against steel woll rubber (Fig. 6S B). Thus, MgF_2-layers manufactured from magnesium ethoxide as precursor evidently outperform the mechanical stability of all so far reported porous MgF_2 layers. In our case, the coatings are remarkably stable. Their mechanical stability was investigated by scratching with steel wool. Usually fine steel wool 0000 is used for this test. The coatings showed very good results, almost no scratches were observed. To achieve a better differentiation in this test, coarse steel wool 00 was used instead. This is a higher mechanical stress for the coatings. The quality of the coatings after this test was judged by comparison with reference samples (see experimental section for details). Results are shown in Figure 12. The coatings are very durable, especially on float glass. Remarkably, the mechanical stability of the coating using aged sols is not worse than in the case of fresh sols. The coatings of borosilicate glass are slightly less mechanically stable.

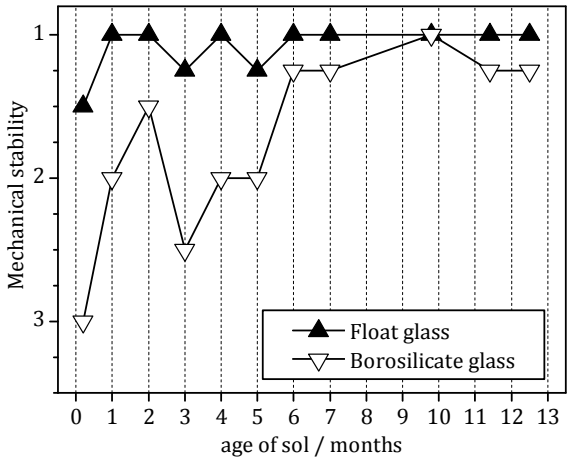

Figure 12. Mechanical stability of the coating using an aged Sol-05A. 1: very good, 3: medium, 5: very bad (see Table 1 for details).

The reasons for this high scratch resistance are not fully understood. But it is quite clear that the calcium content has a great effect. As discussed in the previous section, the sols contain nanoscale MgF_2, CaF_2 and *meta*-$CaMgF_4$ (Figure 5). Upon thermal treatment, pure MgF_2 and CaF_2 with different crystal structures are formed. The scratch resistance of pure MgF_2 layers, containing only uniform particles, is much less pronounced. Probably, the existence of two different types of particles, namely MgF_2 and CaF_2, is the crucial

point to increase the mechanical stability by enforcing thermal densification due to an improved sintering effect. Therefore, the addition of calcium precursors to the reaction mixture was a giant leap forward towards application of porous coating layers made of MgF_2.

7 Summary & Conclusions

Water-clear sols of *nano*-MgF_2 of low viscosity and particle diameters below 10 nm, which possess a remarkably high long-time stability for more than one year, have been synthesized from commercially available magnesium ethoxide $Mg(OEt)_2$ using two different methods.

In the first method, which we call the *CO_2 approach*, CO_2 is bubbled through to a suspension of $Mg(OEt)_2$ in methanol or ethanol. This leads to the formation of clear solutions of magnesium alkylcarbonates. The fluorination of these solutions with anhydrous HF leads to the formation clear MgF_2 sols. This is straightforward in methanol. In ethanol, clear sols may be only obtained, when the HF is solved in *methanol*, and additionally, trifluoroacetic acid is used as additive. A disadvantage of this method is the fact that stoichiometric amounts of CO_2 are necessary.

The second approach, which we call the *chloride approach*, is more universal. As co-reagent, the soluble metal chlorides $MgCl_2$ or $CaCl_2$ (5…30 mol-% of total metal content) are used. During the synthesis, water-free HCl is formed, which functions as a catalyst. This allows the synthesis of water-clear magnesium fluoride sols in ethanol in a one-pot reaction one a 5 liter scale within one day. A major advantage over the CO_2 method is the fact that only stoichiometric amounts of metal chloride are necessary.

The synthesis is quite robust. Although the reactant $Mg(OEt)_2$ is moisture sensitive and should be stored under inert gas, it is sufficient to store it closed to prevent the access of moist air. For practical work, it can be handled at the normal air. Even a partially hydrolyzed product can be used as long as the exact Mg content is known.

The usability of these sols for manufacturing antireflective porous coating with a refractive index of 1.26 has been demonstrated. These porous coating possess high mechanical stability toward scratching with coarse steel wool. This fact is surprising, since porous coatings are usually only of medium mechanical stability. The sol used for the coating application could be stabilized by the addition of a small amount of $Al(O^iPr)_3$. Such a sol was stable for one year under working conditions. Therefore, these sols could serve as a potential new tool in the production of antireflective coatings.

8 Acknowledgements

PD Dr. Gudrun Scholz is gratefully acknowledged for measuring ^{19}F and ^{27}Al NMR spectra of the sols. M. Sc. Dorota Bartkowiak is gratefully acknowledged for measuring TEM images and EDX data.

9 References

1. M. J. Dodge, *Appl. Opt.*, 1984, **23**, 1980-1985.

2. R. K. Iler, *The Chemistry of Silica: Solubility, Polymerization, Colloid and Surface Properties and Biochemistry of Silica*, Wiley, New York, 1979.
3. C. J. Brinker and G. W. Scherer, *Sol-Gel Science - The Physics and Chemistry of Sol-Gel Processing*, Academic Press, Inc., Boston, 1990.
4. T. Schneller and D. Griesche, in *Chemical Solution Deposition of Functional Oxide Thin Films*, eds. T. Schneller, R. Waser, M. Kosec and D. Payne, Springer, Heidelberg, 2013, pp. 29-50.
5. L. Martinů, H. Biederman and L. Holland, *Vacuum*, 1985, **35**, 531-535.
6. D. Jacob, F. Peiró, E. Quesnel and D. Ristau, *Thin Solid Films*, 2000, **360**, 133-138.
7. W. Glaubitt and P. Löbmann, *J. Eur. Ceram. Soc.*, 2012, **32**, 2995-2999.
8. P. Löbmann, in *Chemical Solution Deposition of Functional Oxide Thin Films*, eds. T. Schneller, R. Waser, M. Kosec and D. Payne, Springer, Heidelberg, 2013, pp. 707-724.
9. S. Rüdiger and E. Kemnitz, *Dalton Trans.*, 2008, 1117-1127.
10. E. Kemnitz and J. Noack, *Dalton Trans.*, 2015, **44**, 19411-19431.
11. H. Krüger, E. Kemnitz, A. Hertwig and U. Beck, *Thin Solid Films*, 2008, **516**, 4175-4177.
12. J. Noack, F. Emmerling, H. Kirmse and E. Kemnitz, *J. Mater. Chem.*, 2011, **21**, 15015-15021.
13. J. Noack, K. Scheurell, E. Kemnitz, P. Garcia-Juan, H. Rau, M. Lacroix, J. Eicher, B. Lintner, T. Sontheimer, T. Hofmann, J. Hegmann, R. Jahn and P. Lobmann, *J. Mater. Chem.*, 2012, **22**, 18535-18541.
14. M. Karg, G. Scholz, R. Konig and E. Kemnitz, *Dalton Trans.*, 2012, **41**, 2360-2366.
15. K. Scheurell, J. Noack, R. König, J. Hegmann, R. Jahn, T. Hofmann, P. Löbmann, B. Lintner, P. Garcia-Juan, J. Eicher and E. Kemnitz, *Dalton Trans.*, 2015, **44**, 19501-19508.
16. K. Scheurell, E. Kemnitz, P. Garcia-Juan, J. Eicher, B. Lintner, J. Hegmann, R. Jahn, T. Hofmann and P. Löbmann, *J. Sol-Gel Sci. Technol.*, 2015, **76**, 82-89.
17. T. Murata, H. Ishizawa and A. Tanaka, *Appl. Opt.*, 2008, **47**, C246-C250.
18. F. Chi, G. Wei, Q. Zhang, X. Sun, L. Zhang, X. Lu, L. Wang, F. Yi and X. Gao, *Appl. Surf. Sci.*, 2015, **356**, 593-598.
19. F. Chi, Q. Zhang, L. Zhang, G. Wei, L. Wang and F. Yi, *Mater. Lett.*, 2015, **150**, 28-30.
20. *Germany Pat.,* EP 0 597 210 A1, 1994.
21. W. Behrendt, G. Gattow and M. Dräger, *Z. Anorg. Allg. Chem.*, 1973, **397**, 237-246.
22. J. Kenar, G. Knothe and A. Copes, *J. Amer. Oil Chem. Soc.*, 2004, **81**, 285-291.
23. G. R. Fulmer, A. J. M. Miller, N. H. Sherden, H. E. Gottlieb, A. Nudelman, B. M. Stoltz, J. E. Bercaw and K. I. Goldberg, *Organometallics*, 2010, **29**, 2176-2179.
24. G. Scholz, S. Breitfeld, T. Krahl, A. Düvel, P. Heitjans and E. Kemnitz, *Solid State Sci.*, 2015, **50**, 32-41.
25. G. Scholz, C. Stosiek, J. Noack and E. Kemnitz, *J. Fluorine Chem.*, 2011, **132**, 1079-1085.
26. A. Adam and V. Cirpus, *Z. Anorg. Allg. Chem.*, 1994, **620**, 1702-1706.
27. M. Kunert, P. Wiegeleben, H. Görls and E. Dinjus, *Inorg. Chem. Commun.*, 1998, **1**, 131-133.

28. H. Siebert, *Anwendungen der Schwingungsspektroskopie in der Anorganischen Chemie*, Springer-Verlag, Berlin-Heidelberg-New York, 1966.
29. I. H. Malitson, *Appl. Opt.*, 1963, **2**, 1103-1107.

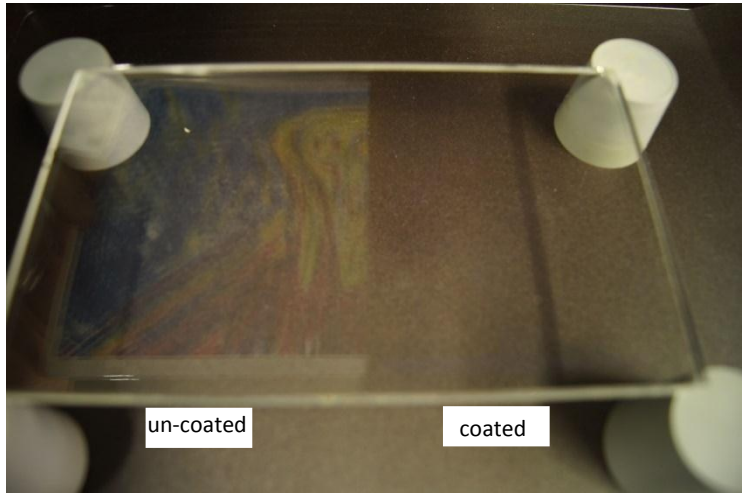

Antireflective coatings were obtained from clear, transparent MgF_2-sols prepared according the non-aqueous fluorolytic sol-gel synthesis